Thermochimica Acta 510 (2010) 9–16

Contents lists available at ScienceDirect

Thermochimica Acta

journal homepage: www.elsevier.com/locate/tca

Kinetics and enthalpy of nitroglycerin evaporation from double base propellants by isothermal thermogravimetry

Muhamed Sućeska*, Sanja Matečić Mušanić, Ivona Fiamengo Houra

Laboratory for Thermal Analysis, Brodarski Institute – Marine Research & Advanced Technologies, Av. V. Holjevac 20, 10020 Zagreb, Croatia

ARTICLE INFO

Article history:
Received 2 February 2010
Received in revised form 14 May 2010
Accepted 16 June 2010
Available online 22 July 2010

Keywords:
Double base
Enthalpy of evaporation
Evaporation
Kinetics of evaporation
Nitroglycerin
Propellants
Thermogravimetry

ABSTRACT

Double base propellants are composed of two basic components: nitrocellulose as a matrix and nitroglycerin as a plasticizer and blasting oil at the same time, and of additives such as stabilizers, burning catalysts, modifiers of ballistic properties, etc.

In the course of time, a number of chemical and physical processes (e.g. stabilizer consumption, migration and evaporation of nitroglycerin, decomposition of nitroglycerin and nitrocellulose, etc.) take place in a propellant grain. The result is a change of propellants' physical, chemical, thermal, ballistic and mechanical properties. The final consequence is reduction of performances and decrease of safe service lifetime of propellants. Reduction of mechanical properties of a propellant grain during ageing can be the factor that limits rockets safe service time. On the other hand, the change in amount of nitroglycerin significantly affects mechanical properties. This is the reason why the evaporation of nitroglycerin from double base propellants is a subject of great importance.

In this work we have studied a very early stage of evaporation of nitroglycerin from a double base rocket propellant applying isothermal thermogravimetry experiments. The experiments were done with a propellant containing 27% nitroglycerin, using thin plate samples having a thickness of 0.2–0.4 mm and weighing ~4 mg.

It was found that at a very early stage the evaporation can be described by the zero-order reaction model, while the entire process is characterized by power law decrees of the evaporation rate with time. The Langmuir vaporization equation, and equations proposed by Pieterse and Focke, and by Beverley et al. are used to relate nitroglycerin mass loss data and the vapor pressure.

The activation energy of nitroglycerin evaporation was calculated to be 81.9 kJ mol^{-1} and the pre-exponential factor 5.6×10^7 s^{-1}, while calculated enthalpy of nitroglycerin evaporation at 298.15 K lies between 80.0 and 90.5 kJ mol^{-1}, depending on the calculation method applied.

1. Introduction

Double base (DB) propellants consist of nitroglycerin (NG) physically entrapped into fibrous nitrocellulose (NC) structure. Nitroglycerin acts as plasticiser and energetic component at the same time. In the course of time, a number of chemical and physical processes (including stabilizer consumption, migration and evaporation of NG, decomposition of NG and NC, etc.) take place in propellant grains. These processes cause changes of physical, chemical, thermal, ballistic, and mechanical properties of propellants, i.e. change of their performances.

In previous studies [1,2] we have shown that mechanical properties of DB propellants significantly change with ageing and can be crucial for their safe service time. Since the amount of NG in the propellant strongly influences its mechanical properties, study of NG evaporation is of great importance.

Tompa [3] has studied evaporation kinetics of NG from DB propellant applying isothermal thermogravimetry and using samples weighing 15–60 mg. He has found that the rate of evaporation depends on the physical state of the propellant; sample size and shape, atmospheric environment, ageing time and crosslink density of propellant, etc. For example, he has found that the evaporation rate increases with the sample's surface area—the larger surface area of the sample, the more NG there is on the surface, and consequently it will evaporate at a faster rate. Also, he has found that the rate of evaporation is higher in helium than in nitrogen or atmospheric air. Tompa has shown that the evaporation rate decreases with crosslink density. The reason is a greater physical entrapment of NG in the case of higher crosslink density, and hence more

---

* Corresponding author. Present address: Energetics Research Institute, Nanyang Technological University, 50 Nanyang Avenue, Block N1-B4a-02, Singapore 639798, Singapore.
E-mail address: suceska@hrbi.hr (M. Sućeska).

0040-6031/$ – see front matter © 2010 Elsevier B.V. All rights reserved.
doi:10.1016/j.tca.2010.06.014

difficult for NG to migrate and reach the surface of the propellant. This influence is more pronounced in the case of larger cylindrical samples (3 mm × 3 mm, 60 mg) than in the case of powdered samples (15 mg).

Tompa has found that in the range of 30–70% mass loss the evaporation of NG can be described by the first-order kinetic model. He reported that the activation energy of NG evaporation in nitrogen atmosphere for cylindrical samples ranges between 57.78 and 80.3 kJ mol^{-1}, and pre-exponential factor between 1.56×10^5 and 3.65×10^6 s^{-1}, depending on NC polymeric matrix crosslink density. For powdered samples he found that the activation energy was the same regardless atmospheric surrounding and crosslink density and equals 75 kJ mol^{-1}, while the pre-exponential factor varies between 2.7×10^6 and 3.7×10^6 s^{-1}. On the basis of his study, Tompa concluded that the mechanism of NG evaporation in powdered samples is thermal transport, while in the case of cylindrical samples NG evaporation is diffusion limited.

Pai Verneker and Kishore [4] have also shown that the decomposition behavior of block samples and powdered samples of DB propellant is different. The difference is due to the occurrence of exothermic NG decomposition in the case of block samples, and NG evaporation in the case of powdered samples. In block samples NG evaporates too, but it has to diffuse through the NC polymeric matrix before it leaves the sample. The diffusion, which is rate-limiting process, involves a definite time and therefore NG can undergo decomposition in the block. However, in powdered samples evaporation and diffusion are closely linked.

Miroschnichenko et al. [5] studied the enthalpy of NG evaporation. The authors measured the enthalpy of evaporation of pure NG by a Calvet microcalorimeter at 40–120 °C temperature range. They expressed the temperature dependence of the enthalpy of evaporation by the equation:

$$\Delta H_{vap} = 98.36 - 0.217T \tag{1}$$

were ΔH_{vap} (in kJ mol^{-1}) is the enthalpy of evaporation of NG, and T is the temperature (in °C). It follows from this dependence that the enthalpy of evaporation of NG at 25 °C equals 92.0 ± 2.1 kJ mol^{-1}, and at the normal boiling point of 250 °C it equals 44.1 kJ mol^{-1}.

Since 1999 a number of authors have reported the use of thermogravimetry for studying the evaporation process. Price and Hawkins [6], and then a series of other authors [7–21], used thermogravimetry to determine the vapor pressure and/or the enthalpy of evaporation of various substances. The application of TGA is based on the fact that all processes accompanied by the mass loss (such is evaporation) can be studied by following the sample mass loss rate as a function of temperature, and applying different equations which relate the mass loss rate and the vapor pressure.

In majority of studies [6–18] determination of the vapor pressure and the enthalpy of evaporation is based on application of the Langmuir equation for free evaporation into vacuum [6]:

$$-\frac{dm}{dt} = p\alpha_{vap} S\sqrt{\frac{M}{2\pi RT}} \tag{2}$$

where (dm/dt) is the rate of mass loss, S is the evaporation surface area, p is the vapor pressure, M is the molecular mass of the effusing vapor, R is the gas constant, T is the absolute temperature, and α_{vap} is the vaporization coefficient.

One of the fundamental assumptions of the Langmuir equation is that the vaporization coefficient (α_{vap}) is constant and equal unity. This assumption enables one to write the following relationship between the vapor pressure and the mass loss rate:

$$p = kv \tag{3}$$

where $k = (\sqrt{2\pi R}/a_{vap})$ and $v = [[(-dm/dt)/S]\sqrt{T/M}]$.

Since assumption is that α_{vap} has constant value, the term k should have a constant value too for a given compound. Hence, a plot of p *vs.* v should give a straight line, the slope of which will give value of k. Determining value of k for a calibration compound, Eq. (3) can be used to determine the vapor pressure of a substance.

Price and Hawkins [6] suggested application of the Langmuir equation only in narrow temperature range, since in the case of a material vaporization into flowing gas stream at atmospheric pressure, the vaporization coefficient may no longer be equal to unity. It was shown [11,15,16] that the vaporization coefficient significantly deviate from unity for experiments conducted in the presence of a purge gas. Consequently, the k term in Eq. (3) cannot be viewed as a calibration constant, and Eq. (3) cannot be applied in such form.

To overcome the problem of non-ideal vaporization coefficient, Phang et al. [15,16] proposed a “comparative method” for developing vapor pressure from TGA experiments, based on the Langmuir equation:

$$p_S = p_R\sqrt{\frac{M_R}{M_S}}\left(\frac{(dm/dt)_S}{(dm/dt)_R}\right), \tag{4}$$

where the subscripts R and S refer to reference and sample data, respectively. The vaporization coefficient Phang et al. excluded from Eq. (4) by mathematical manipulation and in this way the problem associated with the vaporization coefficient is avoided [16]. However, their method does not take into account effect of a flowing gas stream, i.e. effect of diffusion of vapor through a stagnant gas layer. To overcome this problem Pieterse and Focke [19] proposed the following vaporization equation for the situation where the evaporation rate is diffusion limited:

$$-\frac{dm}{dt} = \left(\frac{MS}{hRT}\right)pD, \tag{5}$$

where D is temperature dependent diffusion coefficient through a stagnant gas, and h is thickness of a stagnant gas layer.

As follows from Eq. (5), separate knowledge of the diffusion coefficient is required in order to extract the vapor pressure from TGA experiments. Also, it follows from comparison of Eqs. (2) and (5) that the Langmuir vaporization coefficient (α_{vap}) and the diffusion coefficient (D) are connected by expression:

$$\alpha_{vap} = \frac{D}{h}\sqrt{\frac{2\pi M}{RT}} \tag{6}$$

Beverley et al. [20,21] have shown that in gravimetric experiments conducted at higher purge gas flow rates (up to 4000 ml min^{-1}) and larger stagnant gas layer thickness (>10 mm), the evaporation rate is dependent on a purge gas flow rate. To account effect of a purge gas flow rate, the authors proposed the following vaporization equation:

$$-\frac{dm}{dt} = \left(\frac{MS}{hRT}\right)pD\left(1 - \frac{D}{hF/(S_V + D)}\right), \tag{7}$$

where F is volume gas flow rate and S_V is the cross-section area of the sample.

At higher flow rates the right-hand term in Eq. (7) approaches unity and Eq. (7) becomes identical to Eq. (5). To account effect of a purge gas concentration gradient and existence of an upward convection of the gas mixture, which exists in the case of higher vapor pressures, Beverley et al. modified Eq. (7) introducing a correction factor z [21]:

$$-\frac{dm}{dt} = \left(\frac{MSz}{hRT}\right)pD\left(1 - \frac{D}{hF/(S_V + D)}\right) \tag{8}$$

$$\text{where}: z = \left[\frac{p_{atm}}{p}\ln\left(\frac{1}{1 - p/p_{atm}}\right)\right] \tag{9}$$

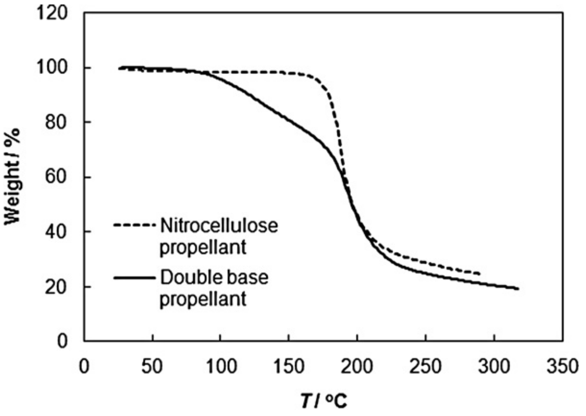

Fig. 1. Non-isothermal TGA curves of NC and DB propellant samples (experimental conditions: heating rate 2° min^{-1}, sample mass 2 mg).

The enthalpy of evaporation can be calculated from known the vapor pressure applying the Clausius–Clapeyron equation [6]:

$$\ln p = B - \frac{\Delta H_{vap}}{RT}, \tag{10}$$

where ΔH_{vap} is the enthalpy of evaporation and B is constant.

The plot of $\ln(p)$ *vs.* $1/T$ will give straight line, slope of which gives value of the enthalpy of evaporation. Assuming constant value of the vaporization coefficient and combining the Langmuir equation (Eq. (3)) and the Clausius–Clapeyron equation (Eq. (10)), the following expression from the calculation of the evaporation enthalpy from the rate of sample mass loss can

$$\ln(v) = B' - \frac{\Delta H_{vap}}{RT} \tag{11}$$

where $B' = [B - \ln(\sqrt{2\pi R}/a_{vap})]$.

Thus, the enthalpy of evaporation can be calculated from by Eq. (11) as a slope of $\ln(v)$ *vs*. $1/T$ plot.

2. Experimental

The evaporation of NG was studied using a DB rocket propellant containing 27% of NG. Isothermal TGA experiments were conducted using thin plate samples weighting around 4.0 mg and having a thickness of 0.2–0.4 mm.

The experiments were done using *TA Instruments* SDT, Model 2960. The samples were tested in open aluminum sample pans having internal diameter of 6 mm and height of 1.2 mm, under nitrogen atmosphere with a flow rate of 50 ml min^{-1}, and in the temperature range 50–100 °C.

3. Results and discussion

3.1. Thermal properties of DB propellants

The non-isothermal TG curve of the studied DB rocket propellant, along with the non-isothermal TG curve of a nitrocellulose (NC) propellant which contains about 98.5% nitrocellulose are given in Fig. 1. It is visible from Fig. 1 that in the case of the NC propellant a measurable mass loss occurs above 150 °C, while in the case of the DB propellant a measurable mass loss is observed above 70 °C.

It was shown by non-isothermal differential scanning calorimetry [22] that there were no measurable exothermal processes for both NC and DB propellants below 140 °C. This means that evaporation of NG can be completely separated from decomposition of NC and NG if temperatures of isothermal experiments are considerably lower than the temperatures of decomposition. To exclude effects of decomposition of NC and DB we have conducted TGA measurements at temperatures below 100 °C (Fig. 2).

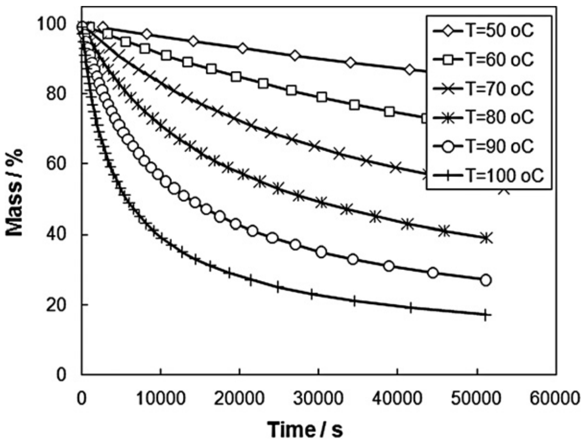

Fig. 2. Isothermal weight loss *vs.* time of tested DB propellant at different temperatures.

The results are in agreement with the results of Tompa [3] and Verneker and Kishore [4] who have found that for powdered samples and at temperatures below 80 °C, the sample mass loss is due to NG evaporation.

3.2. Kinetics of NG evaporation

To study evaporation kinetics of NG, the samples were subjected to isothermal TG experiments at temperatures between 50 and 100 °C. From the sample mass loss-time curves (Fig. 2), the kinetics of evaporation was derived in the following way. The sample mass loss-time data were converted to the fraction evaporated, or conversion (α) *vs.* time, and then to the rate conversion vs. conversion ($d\alpha/dt$ *vs.*α) using formula [23]:

$$\alpha = \frac{m_0 - m_t}{m_0 - m_f} = 1 - \frac{m_t}{m_0 - m_f} \tag{12}$$

where m_0 is the initial sample mass, m_f is the final sample mass, and m_t is the sample mass at a given time.

The conversion is calculated taking that the final sample mass (m_f) is the sample mass after complete evaporation of NG—expressed in percents it equals 73% of the initial sample mass. The obtained ($d\alpha/dt$) *vs.* α data are presented in Fig. 3.

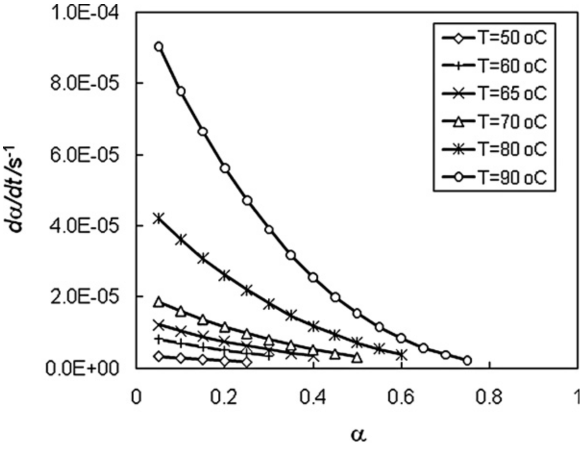

Fig. 3. Conversion rate *vs.* conversion at different temperatures.

Applying differential form of the basic kinetic equation [23]:

$$\frac{d\alpha}{dt} = k_{vap}f(\alpha), \tag{13}$$

where k_{vap} is the evaporation rate constant, and $f(\alpha)$ a function which describes the dependence of the rate of conversion on conversion (so-called reaction model), we found by non-linear regression analysis of $(d\alpha/dt) - \alpha$ data that the evaporation process could be the best described by the n-th order kinetic model (where $n = 2.75$):

$$\frac{d\alpha}{dt} = k_{vap}(1-\alpha)^{2.75} \tag{14}$$

The evaporation rate constants were calculated for each temperature, and then the activation energy (E_{vap}) was calculated from the Arrhenius plot of $\ln(k_{vap})$ *vs.* $1/T$. The obtained values of kinetic parameters are: $E_{vap} = 81.9\,\text{kJ mol}^{-1}$ and $A_{vap} = 5.6 \times 10^7\,\text{s}^{-1}$. This value of the activation energy is close to the values that we obtained by non-isothermal experiments [24]; $E_{vap} = 86$–$93\,\text{kJ mol}^{-1}$. Similar values were obtained also by Tompa [3]—for powdered samples tested in nitrogen atmosphere he obtained $E_{vap} = 75.3\,\text{kJ mol}^{-1}$ and $A_{vap} = 2.7 \times 10^6$–$3.7 \times 10^6\,\text{s}^{-1}$.

We have noted that the exponent n in Eq. (14) is influenced by the sample size and shape (thus we tried to keep the same sample size and shape in all experiments), but the rate constant (k_{vap}) remains unchanged for all samples weighing 2–6 mg. This means that $n = 2.75$ can describe our NG mass loss data (for a given testing-condition), but cannot be used to predict NG mass loss data under different conditions (particularly in the case of larger block samples where diffusion play a role).

3.3. Vapor pressure and enthalpy of evaporation

In double base propellants NG is physically entrapped in the fibrous NC structure. To evaporate the molecules of NG must be located near the sample surface and must have sufficient kinetic energy. At the beginning of evaporation only those molecules of NG located near the sample surface begin to evaporate after being heated. However, as the evaporation proceeds, the evaporated NG has to displace from the sample interior to the surface (diffuse) through the fibrous NC structure. At the same time, liquid NG migrates from the sample interior towards the surface. These processes are particularly pronounced in the case of larger block samples.

Since our goal was to study NG free evaporation we limited our analysis to a very early stage of evaporation (at $t \to 0$). Using this approach, along with the fact that we have used very thin samples, we excluded effects of NG migration and diffusion through NC polymeric matrix on NG evaporation rate. As visible from Fig. 4 the dependence of NG mass loss on time at early evaporation stage is linear (i.e. $dm/dt = \text{constant}$), which means that the process follows zero-order kinetic. At the same time it means that the free sample surface area was not changing significantly at this stage. The initial evaporation rates (dm/dt), at different temperatures, were derived from experimentally obtained m–t curves as a slopes of best-fit straight line in the range 0–10% of NG mass loss (Fig. 4).

The enthalpy of NG evaporation was derived applying Eq. (11) and assuming $\alpha_{vap} = \text{constant}$ but different from unity. The rate of NG evaporation was calculated using two different approaches: as a slope of experimentally obtained m–t curves and from experimentally obtained kinetic data. From the slope of $\ln(v)$ *vs.* $1/T$ plot (Eq. (11)), first approach gives $\Delta H_{vap} = 83.37\,\text{kJ mol}^{-1}$ in temperature range 50–100 °C.

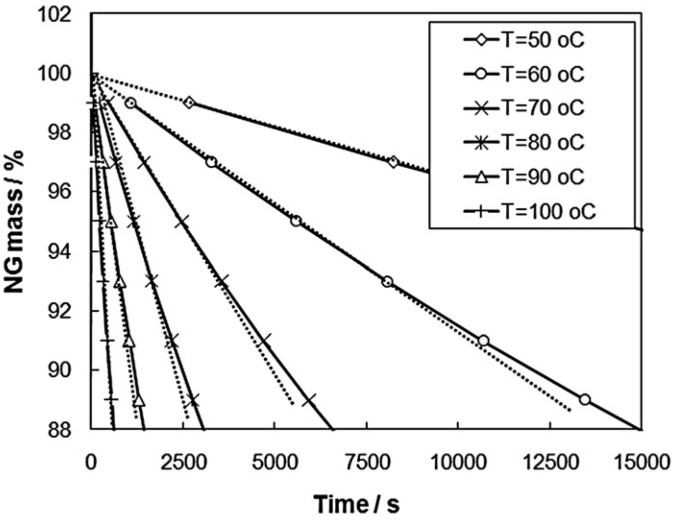

Fig. 4. NG mass loss *vs.* time at initial stage of NG evaporation.

In the second approach the rate of mass loss was substituted by the conversion rate in accordance with Eq. (15).

$$-\frac{dm}{dt} = \Delta m \frac{d\alpha}{dt}, \tag{15}$$

where $\Delta m = m_0 - m_f$.

It follows from Eq. (14), that the initial conversion rate, i.e. the conversion rate at $\alpha = 0$ (i.e. $t = 0$), is equal to the evaporation rate constant (k_{vap}):

$$\frac{d\alpha}{dt} = k_{vap}, \tag{16}$$

which, after substitution into the Langmuir equation, and in combination with the Clausius–Clapeyron equation, gives:

$$\ln(\nu') = B" - \frac{\Delta H_{vap}}{RT} \tag{17}$$

where: $\nu' = (k_{vap}\sqrt{T/M})$

$$B" = B - \ln\left(\frac{\Delta m\sqrt{2\pi R}}{Sa_{vap}}\right)$$

Using experimentally obtained values of $E_{vap} = 81.9\,\text{kJ mol}^{-1}$ and $A_{vap} = 5.6 \times 10^7\,\text{s}^{-1}$, the k_{vap} are calculated for different temperatures in the range 25–250 °C. Then, from the slope of $\ln(\nu')$ *vs.* $1/T$ plot (Eq. (17)), the enthalpy of evaporation was calculated to be $83.51\,\text{kJ mol}^{-1}$, which is almost equal to the values obtained using the first approach. It should be noted that the second approach enables us to extending temperature range beyond temperatures of TGA experiments, assuming the same evaporation mechanism.

The enthalpy of evaporation shows temperature dependence due to the difference in the heat capacity of the liquid and the vapor. This dependence can be expressed by Kirchoff's law:

$$\Delta H_{vap}(T_0) = \Delta H_{vap}(T) + \int_{T_0}^{T} \Delta c_p(T)dT \tag{18}$$

where T_0 is a reference temperature (usually 298.15 K), and Δc_p is difference in heat capacities $[c_p(\text{vapor}) - c_p(\text{liquid})]$.

On the basis of studies conducted on a wide range of materials, Chickos et al. [25] suggested a method for the heat capacity correction to a standard state (or to any temperature):

$$\Delta H_{vap}(T) = \Delta H_{vap}(\overline{T})) + [10.58 + 0.26c_{p,l}(\overline{T} - T)] \tag{19}$$

where $c_{p,l}$ is the heat capacity of liquid at temperature 298.15 K, $\overline{T}$ is a mean temperature at which the determination of H_{vap} was made.

Table 1
Vapor pressure generated from Antoine constants, parameters in Lagmuire equation, and calculated vapor pressure and evaporation enthalpy

T/K	p_A/Pa	$((-dm/dt)/S)$/kg s^{-1}m^{-2}	v	k	α_{vap}	p_L/Pa	Difference between p_A and p_L/%	$\Delta H_{vap,p_L}$/kJ mol^{-1}
298.15	0.07	8.36E−08	3.028E−06	23465.15	3.079E−04	0.08	9.67	83.15
303.15	0.14	1.44E−07	5.266E−06	25977.13	2.782E−04	0.14	−0.94	83.18
313.15	0.46	4.07E−07	1.511E−05	30610.43	2.361E−04	0.39	−15.93	83.22
323.15	1.40	1.08E−06	4.062E−05	34514.09	2.094E−04	1.05	−25.44	83.26
333.15	3.87	2.69E−06	1.030E−04	37541.41	1.925E−04	2.65	−31.45	83.31
343.15	9.81	6.36E−06	2.474E−04	39650.60	1.822E−04	6.37	−35.10	83.35
353.15	23.13	1.43E−05	5.659E−04	40879.49	1.768E−04	14.56	−37.05	83.39
363.15	51.11	3.09E−05	1.237E−03	41318.01	1.749E−04	31.83	−37.72	83.43
373.15	106.57	6.40E−05	2.594E−03	41083.98	1.759E−04	66.76	−37.36	83.47
383.15	211.01	1.27E−04	5.235E−03	40304.53	1.793E−04	134.73	−36.15	83.51
393.15	398.81	2.45E−04	1.020E−02	39103.35	1.848E−04	262.46	−34.19	83.55
403.15	722.82	4.56E−04	1.923E−02	37592.91	1.922E−04	494.80	−31.55	83.60
413.15	1261.36	8.24E−04	3.516E−02	35870.69	2.014E−04	904.91	−28.26	83.64
423.15	2126.73	1.45E−03	6.252E−02	34017.86	2.124E−04	1608.84	−24.35	83.68
433.15	3475.31	2.48E−03	1.083E−01	32099.85	2.251E−04	2786.11	−19.83	83.72
443.15	5519.11	4.14E−03	1.829E−01	30167.77	2.395E−04	4707.97	−14.70	83.76
453.15	8538.68	6.76E−03	3.021E−01	28260.31	2.557E−04	7775.37	−8.94	83.80
463.15	12897.16	1.08E−02	4.884E−01	26405.74	2.736E−04	12569.07	−2.54	83.85
473.15	19055.31	1.70E−02	7.739E−01	24623.82	2.934E−04	19914.43	4.51	83.89
483.15	27587.02	2.61E−02	1.203E+00	22927.57	3.152E−04	30963.79	12.24	83.93
493.15	39195.26	3.94E−02	1.838E+00	21324.72	3.388E−04	47299.60	20.68	83.97
503.15	54727.84	5.87E−02	2.761E+00	19818.98	3.646E−04	71061.49	29.85	84.01
513.15	75192.89	8.59E−02	4.084E+00	18411.05	3.925E−04	105100.65	39.77	84.05
523.15	101773.53	1.24E−01	5.952E+00	17099.47	4.226E−04	153164.95	50.50	84.10

Notes: (dm/dt) calculated from $(d\alpha/dt)$ at $\alpha = 0$ applying Eqs. (14) and (16), $m_f = 4 \times 10^{-6}$ kg, $S = 1.19 \times 10^{-5}$ m^{2}·, p_A is vapor pressure generated from the Antoine constants, p_L is vapour pressure calculated by Eq. (3) using mean value of $k = 25734$, $\Delta H_{vap,p_L}$ is evaporation enthalpy calculated from p_L applying Clausius–Clapeyron equation. All units are expressed in S.I. system.

The enthalpies of NG evaporation at different temperatures are calculated applying Chickos et al. equation and using the mean values of ΔH_{vap} and $\overline{T}$ obtained from two approaches ($\Delta H_{vap,L} = 83.44$ at $\overline{T} = 379$K), and the heat capacity $c_{p,l(NG)} = 295.4$ J mol^{-1} K^{-1} at 298 K [26]. The results of calculations are summarized in Fig. 7.

As mentioned before, the Langmuir equation does not take into account existence of several barriers (influences) to the evaporation process in TGA experiments; influence of purge gas flow rate, diffusion of vapor through a thin layer of a stagnant gas, purge gas concentration gradient in the case of higher vapor pressure, etc. However, despite of the lack of theoretical base some authors demonstrated its applicability in a narrow temperature range [6,10]. In this work we have tested applicability of previously mentioned vaporization equations to describe the evaporation of NG from DB propellants in TGA experiments. For the test we used literature data for the vapor pressure dependence on temperature for pure NG. This dependence is done by the Antoine equation [27]:

$$\log(p) = A - \frac{B}{(T + C)}, \tag{20}$$

where A, B, and C are Antoine constants. According to Yaws et al., when pressure is expressed in mm Hg and temperature in °C the values of the Antoine constants in temperature range 13–406 °C are: $A = 8.323202$, $B = 2305.8$, and $C = 173.838$ [27].

By successive application of experimentally obtained mass loss data, the Antoine and the Langmuir equations, we derived values of k and α_{vap} terms. The term v is calculated using values of NG vapor pressure generated from the Antoine constants (p_A) and NG mass loss rate per unit area ($(dm/dt)S$) derived from experimentally obtained kinetic parameters ($k_{vap} = 5.6 \times 10^7 \exp(-81,900/RT)$ and Eqs. (14) and (15). Then, the k is calculated as a slope of $p_A = vk$ plot. Value of α_{vap} is calculated from $k = (\sqrt{2\pi R}/a_{vap})$. The results of calculation are summarized in Table 1.

It is obvious from Table 1 that the“constant” k changes from 23,465 at 298 K to 41,318 at 363 K (i.e. almost twice), and then decreases again at higher temperatures. The average value of k for temperature range 298–473 equals 25,734. Using this value of k, the Langmuir equation can only roughly reproduce NG vapor pressure in the given temperature range (Fig. 6). At the same time α_{vap} changes from 1.75×10^{-4} at 363 K to 3.08×10^{-4} at 298 K.

Fig. 5 clearly shows that the vapor pressure is not a liner function of the term v in broader temperature range, as it should be according to the Langmuir equation. Only in a narrow temperature range this dependence may be considered linear, which is consistent with Price and Hawkins remark [6]. For example, in temperature range 60–130 °C, the mean value of k equals 39,980 ± 6.8%. This value of k can reproduce the vapor pressure in this temperature range with error less than 6.7%, however outside this temperature range the difference is much higher. The results have confirmed that the Langmuir equation cannot be used for accurate prediction of the vapor pressure in broad temperature range from TGA mass loss data for NG, but for a narrow temperature range it can be used with certain uncertainty, assuming a proper calibration of the constant k.

The values of k and α_{vap} obtained in our study differ for about order of magnitude from the values reported by Chatterjee et al. [11] who obtained for methyl paraben tested under non-isothermal

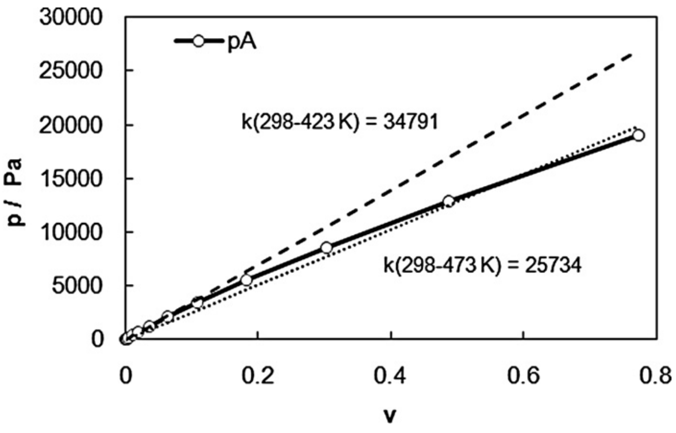

Fig. 5. Vapor pressure *vs.* v in temperature range 298–473 K.

Table 2
Vapor pressure and evaporation enthalpy calculated by Pieterse and Focke vaporization equation.

T/K	p_A/Pa	$((-dm/dt)/S)$/kg s^{-1} m^{-2}	D_C/m^2 s^{-1}	D_F/m^2 s^{-1}	p_P/Pa	Difference between p_A and p_P/%	$\Delta H_{vap,pp}$ /kJ mol^{-1}
298.15	0.07	8.356E−08	1.16E−05	5.53E−06	0.15	108.98	79.78
303.15	0.14	1.441E−07	1.05E−05	5.90E−06	0.25	84.58	79.72
313.15	0.46	4.068E−07	9.08E−06	6.68E−06	0.69	49.93	79.65
323.15	1.40	1.077E−06	8.18E−06	7.51E−06	1.79	27.44	79.58
333.15	3.87	2.688E−06	7.64E−06	8.38E−06	4.35	12.44	79.51
343.15	9.81	6.364E−06	7.34E−06	9.29E−06	10.04	2.30	79.44
353.15	23.13	1.435E−05	7.22E−06	1.02E−05	22.08	−4.55	79.37
363.15	51.11	3.093E−05	7.24E−06	1.12E−05	46.48	−9.06	79.30
373.15	106.58	6.398E−05	7.38E−06	1.22E−05	93.96	−11.83	79.23
383.15	211.01	1.274E−04	7.63E−06	1.33E−05	182.99	−13.28	79.16
393.15	398.82	2.451E−04	7.96E−06	1.44E−05	344.29	−13.67	79.09
403.15	722.84	4.563E−04	8.39E−06	1.55E−05	627.43	−13.20	79.02
413.15	1261.38	8.242E−04	8.90E−06	1.66E−05	1110.13	−11.99	78.95
423.15	2126.76	1.448E−03	9.50E−06	1.78E−05	1910.98	−10.15	78.87
433.15	3475.36	2.478E−03	1.02E−05	1.90E−05	3206.62	−7.73	78.80
443.15	5519.20	4.141E−03	1.10E−05	2.02E−05	5254.14	−4.80	78.73
453.15	8538.81	6.762E−03	1.18E−05	2.14E−05	8419.88	−1.39	78.66
463.15	12897.36	1.081E−02	1.28E−05	2.26E−05	13215.71	2.47	78.59
473.15	19055.59	1.695E−02	1.39E−05	2.39E−05	20343.75	6.76	78.52
483.15	27587.44	2.608E−02	1.51E−05	2.51E−05	30750.70	11.47	78.45
493.15	39195.84	3.943E−02	1.64E−05	2.64E−05	45692.75	16.58	78.38
503.15	54728.66	5.865E−02	1.78E−05	2.77E−05	66811.97	22.08	78.31
513.15	75194.02	8.590E−02	1.93E−05	2.90E−05	96224.83	27.97	78.24

D_C is diffusion coefficient derived by Eq. (6) from known vapor pressure (generated from Antoine constants) and experimental mass loss data, D_F is diffusion coefficient calculated by Eq. (21) using $D_0 = 5.53 \times 10^{-6}$ m^2 s^{-1} and $n = 1.85$, $h = 9 \times 10^{-4}$ m (and taken to be constant at iinitial evaporation stage), p_P is vapor pressure calculated by Eq. (6), $\Delta H_{vap,p_P}$ is evaporation enthalpy calculated from p_p applying Clausius–Clapeyron equation.

conditions in nitrogen atmosphere and with 100 ml min^{-1} flow rate that k = 1,25,452 and $\alpha_{vap} = 5.8 \times 10^{-5}$ (all units in S.I. system). Similar values are reported also by Phang and Dollimore [15] who found for butylated hydroxytoluene tested under non-isothermal conditions in nitrogen atmosphere with 100 ml min^{-1} flow rate values k = 1,23,600 and $\alpha_{vap} = 5.82 \times 10^{-5}$.

The applicability of the vaporization equation proposed by Pieterse and Focke (Eq. (6)), and equation proposed by Beverley et al. (Eq. (8)) are tested using similar approach. From the vapor pressure values generated from the Antoine constants, and from the rate of NG mass loss data obtained from kinetic parameters, parameters in Eqs. (6) and (8) (the correction factor z, the correction term for gas flow rate $(1 - D/(hF/S_V + D))$, and the diffusion coefficient) are calculated. Then, the vapor pressure is calculated from NG mass loss rate and temperature dependent diffusion coefficient. To describe temperature dependence of the diffusion coefficient we used simple power law expression [28,29]:

$$D = D_0 \left(\frac{T}{T_0}\right)^m \frac{p_t}{p_0} \tag{21}$$

Table 3
Vapor pressure and evaporation enthalpy calculated by Beverley et al. vaporization equation

T/K	p_A/Pa	$((-dm/dt)/S)$/kg s^{-1} m^{-2}	D_C/m^2 s^{-1}	D_F/m^2 s^{-1}	Z	t_D	p_B/Pa	Difference between p_A and p_B/%	$\Delta H_{vap,pB}$ /kJ mol^{-1}
298.15	0.071	8.356E−08	1.258E−05	5.53E−06	1.000	0.96	0.15	117.15	79.95
303.15	0.137	1.441E−07	1.137E−05	5.90E−06	1.000	0.96	0.26	92.02	79.91
313.15	0.462	4.068E−07	9.702E−06	6.68E−06	1.000	0.96	0.72	56.35	79.86
323.15	1.402	1.077E−06	8.682E−06	7.51E−06	1.000	0.96	1.87	33.23	79.81
333.15	3.866	2.688E−06	8.071E−06	8.38E−06	1.000	0.95	4.56	17.84	79.75
343.15	9.811	6.364E−06	7.738E−06	9.29E−06	1.000	0.95	10.54	7.48	79.70
353.15	23.132	1.435E−05	7.607E−06	1.02E−05	1.000	0.95	23.26	0.54	79.64
363.15	51.110	3.093E−05	7.632E−06	1.12E−05	1.000	0.95	49.09	−3.96	79.58
373.15	106.574	6.398E−05	7.787E−06	1.22E−05	1.001	0.94	99.47	−6.66	79.50
383.15	211.011	1.274E−04	8.053E−06	1.33E−05	1.001	0.94	194.16	−7.99	79.40
393.15	398.811	2.451E−04	8.421E−06	1.44E−05	1.002	0.94	366.01	−8.23	79.26
403.15	722.824	4.563E−04	8.883E−06	1.55E−05	1.004	0.94	667.87	−7.60	79.05
413.15	1261.361	8.242E−04	9.433E−06	1.66E−05	1.006	0.93	1181.97	−6.29	78.75
423.15	2126.731	1.448E−03	1.006E−05	1.78E−05	1.011	0.93	2031.85	−4.46	78.29
433.15	3475.312	2.478E−03	1.077E−05	1.90E−05	1.018	0.93	3396.37	−2.27	77.61
443.15	5519.112	4.141E−03	1.152E−05	2.02E−05	1.029	0.92	5523.45	0.08	76.58
453.15	8538.679	6.762E−03	1.230E−05	2.14E−05	1.045	0.92	8738.23	2.34	75.04
463.15	12897.165	1.081E−02	1.306E−05	2.26E−05	1.071	0.92	13433.93	4.16	72.70
473.15	19055.309	1.695E−02	1.372E−05	2.39E−05	1.109	0.92	20021.80	5.07	69.04
483.15	27587.021	2.608E−02	1.416E−05	2.51E−05	1.170	0.91	28790.92	4.36	62.99
493.15	39195.257	3.943E−02	1.418E−05	2.64E−05	1.269	0.91	39568.92	0.95	51.90
503.15	54727.839	5.865E−02	1.344E−05	2.77E−05	1.448	0.91	50889.02	−7.01	26.10
513.15	75192.888	8.590E−02	1.125E−05	2.90E−05	1.854	0.90	57443.06	−23.61	

Legend: D_C is diffusion coefficient derived by Eq. (8) from known vapor pressure (generated from the Antoine constants) and experimental mass loss data, D_F is diffusion coefficient calculated by Eq. (21) using $D_0 = 5.53 \cdot 10^{-6}$ m^2 s^{-1} and $n = 1.85$, $t_D = \left(1 - D/(hF/S_V + D)\right)$ is correction term for a purge gas flow rate, $F = 8.33 \cdot 10^{-7}$ m^3 s^{-1}, $S_V = 5.3 \cdot 10^{-6}$ m^2, p_B is vapor pressure calculated by Eq. (8), $\Delta H_{vap,pB}$ is evaporation enthalpy calculated from p_B applying Clausius–Clapeyron equation.

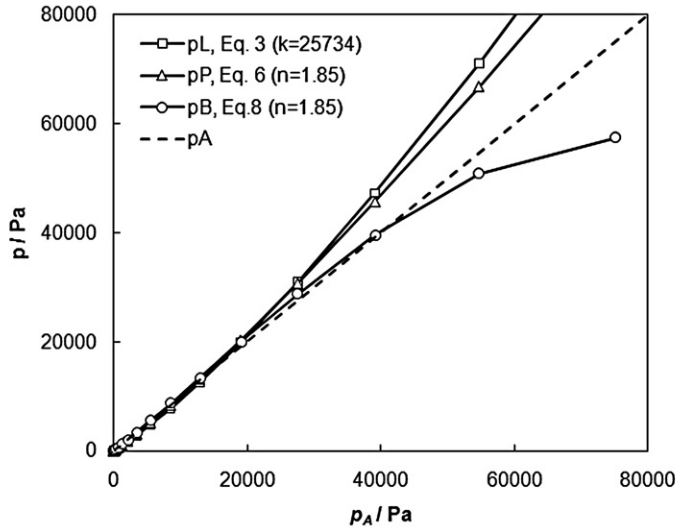

Fig. 6. NG vapor pressure generated from Antoine constants *vs.* vapor pressure calculated by different vaporization equations (p_A: generated from Antoine constants, p_L: calculated by Langmuire equation using $k = 25{,}734$, p_P: calculated by Pieterse and Focke equation, p_B: calculated by Beverley et al.

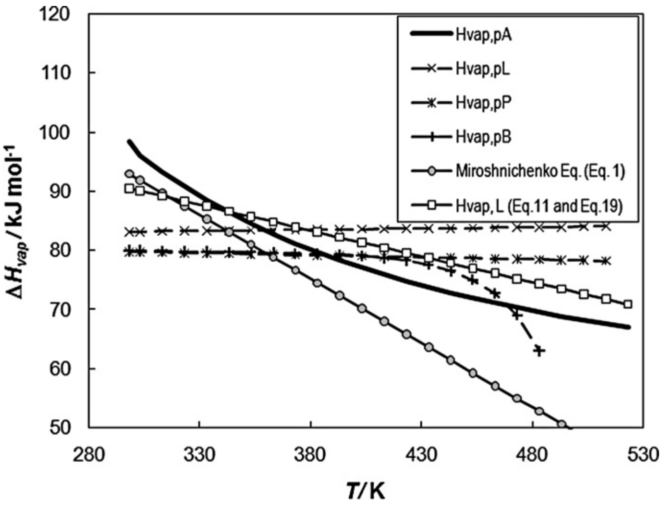

Fig. 7. Calculated evaporation enthalpies of NG *vs.* temperature ($\Delta H_{vap,p_A}$, H_{vap,p_L}, H_{vap,p_P}, $H_{vap,pB}$—calculated from vapor pressure and Clasius–Clapeyron equation, $H_{vap,L}$—calculated from NG mass loss data using Eq. (11), and using temperature corrections given by Eq. (19)).

where T_0 and p_0 are reference temperature and pressure respectively, p_t is the total pressure, D_0 is the diffusion coefficient at reference conditions, and m is exponent (which in accordance with the kinetic theory of gases equals 3/2 [26]).

In the calculation we used literature value for the diffusion coefficient at 298 K and 1 bar; $D_0 = 5.53 \times 10^{-6}\,\mathrm{m^2\,s^{-1}}$ [26], and then adjusted exponent n to obtain the best agreement between the calculated vapor pressure and the vapor pressure generated from the Antoine constants. The pressure p_t is assumed to be atmospheric. The results of calculation are summarized in Tables 2 and 3 and in Fig. 6.

It follows from Tables 2 and 3 that the values of diffusion coefficients derived from p_A and mass loss data (D_C) lie between 1.9×10^{-5} and $7 \times 10^{-6}\,\mathrm{m^2\,s^{-1}}$, in temperature range 298–520 K. These values are slightly higher than the value reported in literature; $D = 5.53 \times 10^{-6}\,\mathrm{m^2\,s^{-1}}$ at 298 K, for diffusion of NG in air or nitrogen [26]. Also, one may note that the calculated diffusion coefficient shows unusual temperature dependence—it decreases from 298 K to 373 K and that increases from 373 K to higher temperatures. Because such dependence cannot be described satisfactory by Eq. (21), we have derived exponent m using the literature value for D_0 and adjusting it until the best agreement between p_A, and p_B and p_P was obtained. In this way we obtained $m = 1.85$. This value of m gives satisfactory agreement between D_C and D_F at higher temperatures, in the temperature range 330–500 K. Also, this value of m is close to value predicted by kinetic theory of gases ($m = 3/2$) [28], and values reported for binary diffusion coefficients of some gases; $m \sim 1.7$ [29] and $m = 1.82$–2.2 [30].

Beverley et al. [20] have noted that it is not clear what value of S_V should be used—total cross-section area of the sample tube (i.e. sample), or area of the sample vessel minus area of the sample. The authors have found that both approaches give almost the same results. We have found that better results were obtained if we use S_V to be equal to upper sample surface area. Hence in our calculations we used S_V equals the upper sample surface area.

Tables 1 and 2, and Fig. 6, show that none of tested vaporization equations cannot reproduce accurately NG vapor pressure generated from the Antoine constants in broad temperature range between the room temperature and the boiling temperature (520 K). The Langmuir equation, with average value of $k = 25{,}734$, gives the vapor pressures which significantly differs from the vapor pressure generated from the Antoine constants. The Pieterse and Focke equation gives better agreement in temperature range 340–500 K—difference is below 15%. Outside this temperature range the difference is much higher (Table 2). The Beverley et al. equation gives the best agreement among these three vaporization equations—in temperature range 340–500 K the difference is below 9%, however outside these limits the difference is much larger. It should be mentioned that all tested equations fail to predict accurately the vapor pressures at lower temperatures (below 333 K)—the difference can be more than 100%.

The Pieterse and Focke equation gives higher values of the vapor pressure at higher temperatures, i.e. higher pressures. As the author mentioned, the equation is applicable for diffusion control evaporation through a stagnate gas, but at lower vapor pressures. The Beverley et al. equation, which includes corrections for higher vapor pressures (the correction factor z), and the correction for gas flow rate (the right-hand term in Eq. (8), t_D), gives better agreement in the range of moderate values of the vapor pressures. At higher vapor pressures, above 5×10^4 Pa, the Beverley et al. equation gives lower values of calculated vapor pressures. This is probably the consequence of inability of Eq. (9) to predict accurately the correction for the vapor pressures close to the atmospheric pressure. The conclusion is based on the fact that the vapor pressure generated from Antoine constants shows a monotonic (power law) increase with temperature, even at $p \geq p_{atm}$, however Eq. (9) predicts a fast increase of z as p approaches p_{atm} (as p approaches p_{atm},z approaches infinite value). This results in lower values of calculated vapor pressure.

At the same time it seems that the correction term z, at constant heat flow rates experiments, has the key influence on the vapor pressure derived from TGA experiments. This follows from the fact that a gas flow rate correction term (t_D) does not change too much (from 0.96 to 0.90 for temperature range 298–510 K), and the correction term z was the main parameter that corrects the vapor pressure value at a given temperature (Eq. (8)).

We used calculated values of the vapor pressures (p_L, p_P, and p_B) to derive the evaporation enthalpy of NG as a function of temperature, applying the Clausius–Clapeyron equation (Eq. (10)). The results of calculation, along with the enthalpies of evaporation derived applying Eq. (11) and temperature correction by Eq. (18), are summarized in Fig. 7.

It is visible from Fig. 7 that the enthalpies of NG evaporation calculated from the vapor pressures have almost constant value in temperature range 298–513 K for all vaporization equations tested—the values range between 80 and 83 kJ mol^{-1}. The exception is the evaporation enthalpy calculated from p_B ($H_{vap,pB}$), which shows fast decrease above 450 K. The fact that the calculated evaporation enthalpies considerable differ from the enthalpies derived from the vapor pressure generated from the Antoine constants, and that the evaporation enthalpies do not show expected temperature dependence, indicates inability of these equations to relate the vapor pressure and mass loss rate from TGA experiments with sufficient accuracy.

The evaporation enthalpy calculated from TAG mass loss data and the Langmuir and Clausius–Clapeyron equations, and Chickos et al. equation for temperature corrections, gives a reasonable agreement—the difference between $\Delta H_{vap,p_A}$ and $\Delta H_{vap,L}$ is less than 4 kJ mol^{-1} (< 5%) in whole temperature range, except for the room temperature where difference is 8 kJ mol^{-1} (i.e. 8%).

This work gives slightly lower value of the evaporation enthalpy at 298 K ($\Delta H_{vap,L}$ = 90.5 kJ mol^{-1}) than the value calculated from the Antoine pressure ($\Delta H_{vap,p_A} = 92.9$ kJ mol^{-1}), and slightly higher value at the boiling temperature of 523 K ($\Delta H_{vap,L}$ = 70.6 kJ mol^{-1} and $\Delta H_{vap,p_A} = 66.7$ kJ mol^{-1}). At the same time it seems that the Miroshnichenko et al. equation (Eq. (1)) considerable lover values of the evaporation enthalpy at NG boiling temperature ($\Delta H_{vap,p_A} =$ 44.7 kJ mol^{-1}). The above results show that the Langmuir equation, in combination with the Clausius–Clapeyron equation, can be used to predict the evaporations enthalpy from the mass loss data with the error less than 10%, in spite of the fact that it is not adequate to calculate the vapor pressure from TGA data.

4. Conclusions

We have studied a very early stage of evaporation of nitroglycerin from double base propellant using isothermal thermogravimetry and the vaporization equations which relate the rate of nitroglycerin mass loss and vapor pressure.

The results have shown that at the early stage evaporation follows zero-order kinetics, while at later stage the rate of evaporation decreases due to reduction of the evaporating surface area and effects of migration and diffusion of nitroglycerin toward the sample surface.

It was found out that none of tested vaporization equations (the Langmuir, Pieterse and Focke, and Beverley *et al.* equations) cannot predict accurately the vapor pressure from TGA data in a broad temperature range—from the room temperature to the boiling temperature (298–523 K). The best results were obtained using the Beverley et al. equation, but it seems that more additional work should be done in order to describe accurately effects all barriers/influences to the evaporation process that exist in TGA experiments. In particular it refers to the correction term z in Eq. (8), which plays key role at higher vapor pressures.

The Langmuir equation, which is admittedly not perfect and strictly speaking not applicable to relate the rate of mass loss obtained in TGA experiments and the vapor pressure (since it is derived for the evaporation into vacuum and neglects existence of any barrier and influence to the evaporation process), can still estimate the vapor pressure over a finite temperature and pressure ranges to a some accuracy. The results show that it is possible to estimate the evaporation enthalpy to a good accuracy combining the Langmuir and the Clausius–Clapeyron equations, and using Chickos et al. equation to make the heat capacity corrections. The evaporation enthalpy of NG, derived in this way, equals 90.5 kJ mol^{-1} at 298 K, which is ~8% lower than the enthalpy derived from the vapor pressure generated from the Antoine constants.

References

[1] S. Matečić Mušanić, M. Sućeska, S. Bakija, Applicability of dynamic mechanical and thermal methods in investigation of ageing processes of double based rocket propellants, in: Proc. of 9th Seminar ″New Trends in Research of Energetic Materials″, Pardubice, 2006, pp. 214–230.

[2] S. Matečić Mušanić, M. Sućeska, M. Rajić Linarić, S. Bakija, R. Čuljak, Changes of dynamic mechanic properties of double based rocket propellant during artificial ageing, in: Proc. of 7th Seminar ″New Trends in Research of Energetic Materials″, Pardubice, 2004, pp. 570–583.

[3] A.S. Topma, Thermal analysis of liquid and solid propellants, J. Hazard. Mater. 4 (1980) 95–112.

[4] V.R. Pai Verneker, K. Kishore, Studies on thermal decomposition of double-base propellants, J. Spacecraft 20 (2) (1983) 141–143.

[5] E.A. Miroshnichenko, L.I. Korchatova, V.P. Shelaputina, S.A. Zyuzǐkevich, Yu.A. Lebedev, Thermochemistry of glycerol trinitrate, Bull.Acad. Sci. USSr, Div. Chem. Sci. (1988) 1778–1781.

[6] D.M. Price, M. Hawkins, Vapour pressures of hydroxybenzophenone UV absorbers, Thermochim. Acta 329 (1999) 73–76.

[7] D.M. Price, Vapor pressure determination by thermogravimetry, Thermochim. Acta 367–368 (2001) 253–262.

[8] D.M. Price, Volatilisation, evaporation and vapour pressure studies using a thermobalance, J, Therm. Anal. Calorim. 64 (2001) 315–322.

[9] K. Chatterjee, D. Dollimore, K. Alexander, Calculation of vapour pressure curves for ethyl, propyl,and butyl parabens using thermogravimetry, Instrum, Sci. Technol. 29 (2) (2001) 133–144.

[10] K. Chatterjee, A. Hazra, D. Dollimore, K.S. Alexander, Estimating vapour pressure curves by thermogravimetry: a rapid and convenient method for characterization of pharmaceuticals, Eur. J. Pharm. Biopharm. 54 (2002) 171–180.

[11] K. Chatterjee, D. Dollimore, K. Alexander, A new application for the Antoine equation in formulation development, Int. J. Pharm. 213 (2001) 31–44.

[12] A. Hazra, D. Dollimore, K. Alexander, Thermal analysis of the evaporation of compounds used in aromatherapy using thermogravimetry, Thermochim. Acta 392–393 (2002) 221–229.

[13] T.V. Sorokina, D. Dollimorea, K.S. Alexander, Evaporation of the fragrance component, cinnamyl alcohol, using simultaneous TG–DTA, Thermochim. Acta 392–393 (2002) 315–321.

[14] A. Tatavarti, D. Dollimore, K.S. Alexander, A Thermogravimetric Analysis of Non-polymeric Pharmaceutical Plasticizers: Kinetic Analysis, Method Validation, and Thermal Stability Evaluation, AAPS PharmSci. 4 (4) (2002) 1–11.

[15] P. Phang, D. Dollimore, The calculation of the vapour pressures of antioxidants over a range of temperatures using thermogravimetry, Thermochim. Acta 367–368 (2001) 263–271.

[16] P. Phang, D. Dollimore, S.J. Evans, A comparative method for developing vapor pressure curves based on evaporation data obtained from a simultaneous TG-DTA unit, Thermochim. Acta 392–393 (2002) 119–125.

[17] S.F. Wright, D. Dollimore, J.G. Dunn, K. Alexander, Determination of the vapor pressure curves of adipic acid and triethanolamine using thermogravimetric analysis, Thermochim. Acta 421 (2004) 25–30.

[18] A. Gairola, G.V. Kunte, A.M. Umarji, S.A. Shivashankar, Determination of the enthalpies of sublimation and evaporation from thermogravimetric data: Application to metalorganic complexes of Al and Cr, Thermochim. Acta 488 (2009) 17–20.

[19] N. Pieterse, W.W. Focke, Diffusion-controlled evaporation through a stagnant gas: estimating low vapour pressure from thermogravimetric data, Thermochim. Acta 406 (2003) 191–198.

[20] K.J. Beverley, J.H. Clint, P.D.I. Fletcher, Evaporation rates of pure liquids measured using a gravimetric technique, Phys. Chem. Chem. Phys. 1 (1999) 149–153.

[21] K.J. Beverley, J.H. Clint, P.D.I. Fletcher, Evaporation rates of structured and non-structured mixtures, Phys. Chem. Chem. Phys. 2 (2000) 4173–4177.

[22] I. Fiamengo, M. Sućeska, S. Matečić Mušanić, Applicability of thermal methods for identification of homogeneous propellants, Proc. of 11th Seminar ″New Trends in Research of Energetic Materials″, Pardubice (2008) 513–523.

[23] J. Šestak, Study of the kinetics of the mechanism of solid-state reactions at increasing temperatures, Thermochim. Acta 3 (1971) 1–12.

[24] S. Matečić Mušanić, M. Sućeska, I. Fiamengo, R. Čuljak, Kinetics of nitroglycerin evaporation in double base rocket propellants, in: Proceedings of 11th Seminar ″New Trends in Research of Energetic Materials″, Pardubice, 2008, pp. 642–652.

[25] J. Chickos, A protocol for correcting experimental fusion enthalpies to 298.15 K and it's application indirect measurements of sublimation enthalpy at 298.15 K, Thermochim. Acta 313 (1998) 19–26.

[26] R. Mayer, J. Kohler, A. Homburg, Explosives, Fifth Edition, Wiley-VCH Verlag GmbH & Co. KGaA, Weinheim, 2002, pp. 226.

[27] L. Yaws Carl, K. Narasimhan Prasad, C. Gabbula, Yaws' Handbook of Antoine Coefficients for Vapor Pressure, 2nd electronic edition, Knovel, New York, 2009.

[28] E.M. Nafikov, A.G. Usmanov, Temperature dependence of the diffusion coefficients of gases, J. Eng. Phys. Thermophys. 17 (3) (1969) 1158–1162.

[29] N. Matsunaga, M. Hori, A. Nagashima, Measurement of mutual diffusion coefficients of gases by the taylor method: measurements on H_2–air, H_2–N_2, and H_2–O_2 systems, Heat Transfer - Asian Res. 31 (3) (2002) 182–193.

[30] J.C. Slattery, R.B. Bird, Calculation of the diffusion coefficient of dilute gases and the self-diffusion coefficient of dense gases, AIChE J. 4 (2) (1958) 137–142.